ELSEVIER

Thermochimica Acta 299 (1997) 145–151

thermochimica acta

Vapor-pressure scanning of solids. A novel way to probe non-stoichiometry

Jacob H. Greenberg*

Department of Inorganic and Analytical Chemistry, Hebrew University, Jerusalem 91904, Israel

Abstract

Investigation of non-stoichiometry of important classes of inorganic materials is often hampered by a very narrow ($<$ 0.1 at.%) range of existence of solid phases. A new approach to this problem based on experimental study of *P–T–X* (pressure–temperature–composition) phase equilibrium is discussed. From the vapor-pressure measurements, the space arrangement of the single-phase volumes of the conjugated condensed and vapor phases is reconstructed from a data set of scanning points. It has been shown that standard vapor-pressure equipment makes it possible to directly determine the composition of the condensed phase with an accuracy of up to (10^{-3}–10^{-4}) at.% at high temperature, thus allowing studies of crystals with a sub-0.1 at.% non-stoichiometry range. Results of vapor-pressure scanning of high-T_c superconductor and semiconductor materials are presented.

Keywords: High-T_c superconductors; Non-stoichiometry; Semiconductors; Vapor-pressure scanning

1. Introduction

It has already become kind of a platitude among materials scientists to say that non-stoichiometry is the central problem of materials science. Nevertheless, it should be admitted with a certain measure of embarrassment that until recently there were no adequate experimental ways to probe the non-stoichiometry of solids with a sub-0.1 at.% range of existence under equilibrium conditions with two-component vapor which comprise virtually all the binary semiconductors as well as other materials of technical importance.

In the present paper, a new approach to this problem, known as vapor-pressure scanning [1], is discussed and previously reported results are reviewed.

*Corresponding author. Tel.: 00-972-2-6586-174; fax: 00-972-2-6585-319; e-mail: JACGREEN@vms.huji.ac.il.

PII S0040-6031(97)00171-8

2. Results and discussion

Vapor-pressure scanning is a direct method. In this approach [1] the limit of existence of a binary non-stoichiometric crystal $AB_{1\pm\delta}$ is experimentally registered as a point of phase transition between univariant and bivariant equilibrium. Within the solid–vapor (SV) equilibrium, due to incongruent sublimation, the composition of the solid X_s gradually changes on heating in such a way that in a closed volume v at the temperature T it is determined by the initial masses of the two elements (N_A, N_B) and the evaporated quantities of those elements n_A and n_B:

$$X_s = \frac{N_B - n_B}{(N_A + N_B) - (n_A + n_B)} 100\% \quad (1)$$

The composition of the conjugated vapor X_v

$$X_v = \frac{n_B}{n_A + n_B} 100\% \quad (2)$$

is determined by the total vapor pressure P which is a sum of all partial pressures P_j,

$$P = \sum_j P_j \tag{3}$$

two equations ($i = \mathrm{A}, \mathrm{B}$) representing the mass conservation law for both elements:

$$n_i = (v/RT) \sum_j \mu_{ij} P_j, \quad i = \mathrm{A}, \mathrm{B} \tag{4}$$

(μ_{ij} is the stoichiometric number of the component i for every vapor-phase species j), and the equilibrium constants of all the vapor-phase reactions

$$K_\mathrm{p} = \prod_j P_j^{\nu_{ij}} \tag{5}$$

In Eq. (5) ν_{ij} is the coefficient of the species j in the reaction i.

The system of five equations (Eqs. (1)–(4)) comprises six unknowns: two compositions (X_s and X_v), two n's (n_A and n_B) and two independent partial pressures, since the equilibrium constants, K_p in Eq. (5), reduce the total number of P_j's to only two independent ones. So, in general, the set of Eqs. (1)–(4) is indeterminate and, consequently, cannot be solved. The way to overcome this obstacle was laid out in [1,2]. It has been shown that, if the vapor-pressure experiment is designed so that two different vapor-pressure curves intersect within the same SV range then the composition of the solid at the point of intersection is defined as

$$X_\mathrm{s} = \frac{N_{\mathrm{B},1}\nu_2 - N_{\mathrm{B},2}\nu_1}{(N_{\mathrm{A},1} + N_{\mathrm{B},1})\nu_2 - (N_{\mathrm{A},2} + N_{\mathrm{B},2})\nu_1} 100\% \tag{6}$$

Eq. (6) relates X_s to initial experimental conditions for the two intersecting curves (volumes and initial masses) and involves no information whatsoever about the vapor. It means that Eq. (6) is applicable to an arbitrary composition of the vapor, unknown, in particular. This is an important result which paves the way for determining the composition of the solid X_s independent of the composition of the vapor X_v. A network of vapor-pressure curves, covering the entire region of existence of the solid, results in a data file of intersecting points which scan the whole of the solidus, and from which the solidus surface is reconstructed in the P–T–X phase space. That is why this method was called vapor-pressure scanning of solids. The composition of the conjugated vapor is given by Eqs. (2)–(4) from which activities of the components are readily calculated, resulting in complete thermodynamic characterization of the solid phase.

Eq. (6) points to an additional area of application of vapor-pressure scanning, i.e. characterization of the material, or 'chemical analysis'. If the solidus surface of a certain material has been scanned, then all one has to do to analyze a sample is to measure the vapor pressure for this sample, to find the suitable intersection points and determine the composition of the sample from Eq. (6).

Vapor-pressure scanning has been applied to a number of inorganic materials, some of which are discussed below.

2.1. The Y–Ba–Cu–O system

The details of the experiment have been given elsewhere [3]. The vapor pressure was measured as a function of the temperature for 16 samples of $YBa_2Cu_3O_y$ with different initial oxygen content. An experimental data set comprising 611 scanning points, has been reported earlier [4]. In the temperature range under consideration, the predominant vapor species in equilibrium with $YBa_2Cu_3O_y$ is O_2. The partial pressures of other species are too small to influence the numerical results and can well be neglected in the calculations. It has also been shown [5–10] that, in this P–T–X range, the only condensed phase is $YBa_2Cu_3O_y$, which loses oxygen on heating according to the phase reaction

$$YBa_2Cu_3O_y(\mathrm{s}) \Rightarrow YBa_2Cu_3O_{y-\delta}(\mathrm{s}) + 0.5\delta O_2(\mathrm{g})$$

Consequently, at a fixed cation ratio the system can be considered quasi-binary; one quasi-component being the sum of the metals and the other, oxygen. Oxygen non-stoichiometry in oxides is usually described in terms of oxygen index, or the number of oxygen atoms per formula. In the vapor-pressure experiment, the oxygen index y at every (P,T) point is associated with the initial oxygen index y_0:

$$y = y_0 - 2Pv(a + by_0)/mRT \tag{7}$$

where a is the total molar mass of the metals (Y + 2Ba + 3Cu), b the atomic mass of oxygen,

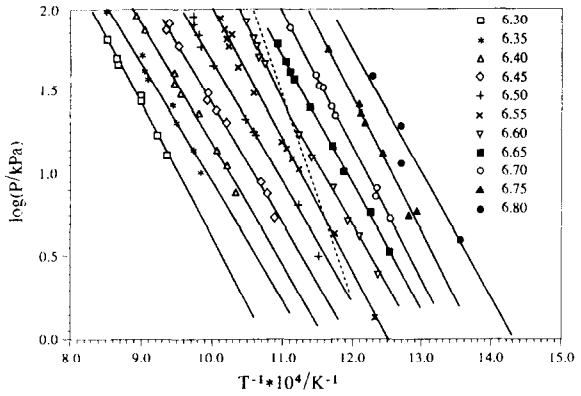

Fig. 1. Temperature dependencies of the oxygen vapor pressure for different oxygen indices in $YBa_2Cu_3O_y$ [3,4]. The dashed line represents the experimental tetragonal ⇔ orthorhombic phase transition.

and m the initial mass of the sample Eq. (6) can be rearranged as follows:

$$Y_{1,2}=\frac{m_1v_2y_{0,1}/(a+by_{0,1})-m_2v_1y_{0,2}/(a+by_{0,2})}{m_1v_2/(a+by_{0,1})-m_2v_1/(a+by_{0,2})} \quad (8)$$

Here, $y_{1,2}$ is the oxygen index of the $YBa_2Cu_3O_y$ phase at the intersection point of two $P(T)$ curves for samples with initial indices $y_{0,1}$ and $y_{0,2}$.

Once the vapor-pressure scanning of the $YBa_2Cu_3O_y$ phase was completed, the P-T-X phase arrangement of the solidus was determined. Fig. 1 shows a number of $X_s = \text{const}$ curves for the $YBa_2Cu_3O_y$ solidus from which thermodynamic functions of oxygen were derived and reported [3].

2.2. Semiconductor materials

2.2.1. CdTe

$YBa_2Cu_3O_y$ is a phase with quite a sizable range of existence, spanning 6-to-7 oxygens per formula. A qualitatively different situation arises when dealing with semiconductors for which the single-phase range of existence is comparable, or even smaller than the possibilities of standard equipment. Fig. 2 is the P–T projection of the CdTe system, which is the first direct experimental measurement of the vapor pressure for CdTe [11,12]. T_{cf} is the congruent melting temperature, T_{cs} the congruent sublimation temperature, T_{max} the maximum melting temperature of the solid. The inset is the melting region both in T–X and P–T

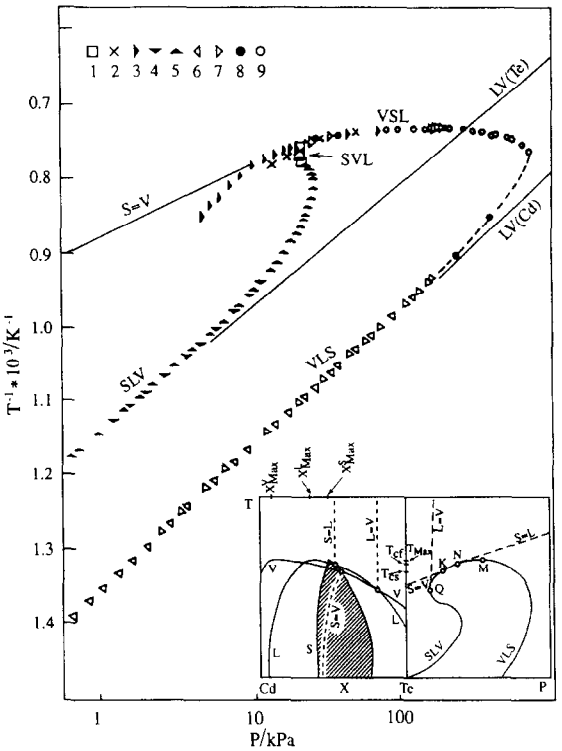

Fig. 2. P–T projection of the CdTe diagram [11,12]. The order of phases in three-phase equilibria such as SLV, VSL, SVL and VLS corresponds to the increase in Te content in phases. Different shapes of experimental points refer to different initial compositions. The S=V curve is given according to [14].

projections. The tip of the solid CdTe is shaded. Two major specifics of this diagram are:

1. At the maximum melting point, T_{max}, the liquid is richer in Cd than the solid, and the vapor is still richer in Cd than both of them;
2. S = V (the vapor-pressure minimum, or the congruent sublimation curve) touches the Te-rich portion of the graph.

The results of the vapor-pressure scanning of the solidus are presented in Fig. 3 and Table 1. Fig. 3 is the T–X projection of the liquidus, vaporus and, under 10 000 magnification, the solidus. The solidus is strongly asymmetrical: maximum Te solubility is ca. 10^{-2} at.%, an order of magnitude greater than that for Cd. At T_{max}, the liquid is slightly enriched in Cd while the vapor is almost pure Cd. This is a consequence of the space arrangement of the congruent

Table 1
Homogeneity limits of CdTe, liquidus and congruent sublimation

T/K	P/kPa	X_s/at.%Te	X_L/at.%Te	X_V/at.%Te
Cd saturated CdTe				
697.2	0.48	50.0002 ± 0.0002	—	0
819.6	4.46	50.0001 ± 0.0001	—	0
864.1	9.09	49.9990 ± 0.0001	—	0
871.3	10.18	49.9983 ± 0.0006	—	0
900.8	15.87	49.9990 ± 0.0001	—	0
939.7	27.87	49.9994 ± 0.0002	—	0
969.4	42.17	49.9991 ± 0.0002	—	0
992.0	57.26	49.9967 ± 0.0003	—	0
1073	146.25	49.9966	—	—
1123	239.98	49.9946	—	—
1173	319.97	49.9957	—	—
1223	379.96	49.9967	—	—
Te saturated CdTe				
945.5	2.33	50.0006 ± 0.0001	—	99.9
1016.6	5.66	50.0036 ± 0.0001	—	99.9
1046.9	7.88	50.0055 ± 0.0004	—	99.9
1073	9.87	50.0071	—	—
1076.0	10.35	50.0073 ± 0.0001	—	99.8
1094.1	12.04	50.0092 ± 0.0003	—	99.9
1103.3	12.98	50.0098 ± 0.0001	—	99.7
1121.0	14.78	50.0138 ± 0.0007	—	99.6
1123	14.80	50.0138	—	—
1173	18.80	50.0135	—	—
1223	19.73	50.0082	—	—
1243.1	21.29	50.0087 ± 0.0008	—	96.5
1282.2	19.72	50.0050 ± 0.0010	—	96.0
1285.5	19.51	50.0047 ± 0.0015	—	90.8
1301.0	18.38	50.0044 ± 0.0030	—	85.6
1312.0	17.47	50.0038 ± 0.0040	—	77.7
1359.4	73.20	50.0034 ± 0.0006	—	2.0
1361.8	87.22	50.0013 ± 0.0004	—	0.8
Liquidus				
1034.8	6.85	—	82.81	100
1124	15.48	—	73.77	99
1176.3	19.53	—	66.86	99
1234.9	21.38	—	61.52	96
1281.3	19.77	—	56.80	91
1336.3	25.16	—	52.62	27
1357.3	63.50	—	50.86	3.5
1364.7	134.79	—	50.0003	0.4
Congruent sublimation				
1073	0.35	50.00079	—	—
1123	0.91	50.00083	—	—
1173	2.15	50.00109	—	—
1223	4.76	50.00150	—	—
1324	19.86	50.00218	—	—

sublimation line (Table 1); at low temperature, it approaches the stoichiometry, whereas at high temperature it inclines considerably toward Te, so that the maximum congruent sublimation temperature T_{cs} is as much as 41 K lower than T_{max}. This is the key issue of the whole CdTe technology. The calculated confidence intervals for X_s depended on individual experimental conditions and were within 10^{-4} at.% (Table 1). If the solidus volume is cut with planes of constant composition and the composition of the conjugated vapor is traced in these planes, then the partial thermodynamic functions of Cd and Te are readily calculated by applying standard thermodynamic procedure. The corresponding results have been reported [13].

2.2.2. Zn_3As_2 and Cd_3As_2

For CdTe, it was shown that the congruent sublimation composition is variable and approaches the stoichiometric plane at low temperatures. Vapor-pressure scanning of different solids proved to be sensitive enough to show that the stoichiometry is as good a composition as any other. For example, in Zn_3As_2 (Fig. 4) [15] the congruent sublimation composition at lower temperatures is on the Zn side of the stoichiometry (39.997 at.% As at 1045 K), crossing the stoichiometric plane on heating up to ca. 1065 K, and ending up on the As side of the stoichiometric plane (40.005 at.% As at 1152 K). It means that in a certain temperature range ($T < 1065$ K), sub-stoichiometric Zn_3As_2 can be in equilibrium with almost pure As vapor, whereas at $T > 1081$ K over-stoichiometric Zn_3As_2 can be in equilibrium with almost pure Zn vapor.

In Cd_3As_2 (Fig. 5), the stoichiometric plane is completely outside the solidus of the low temperature α-polymorph and only touches the solidus volume of the high temperature β-phase [16]. The congruent sublimation compositions for both α- and β-phases

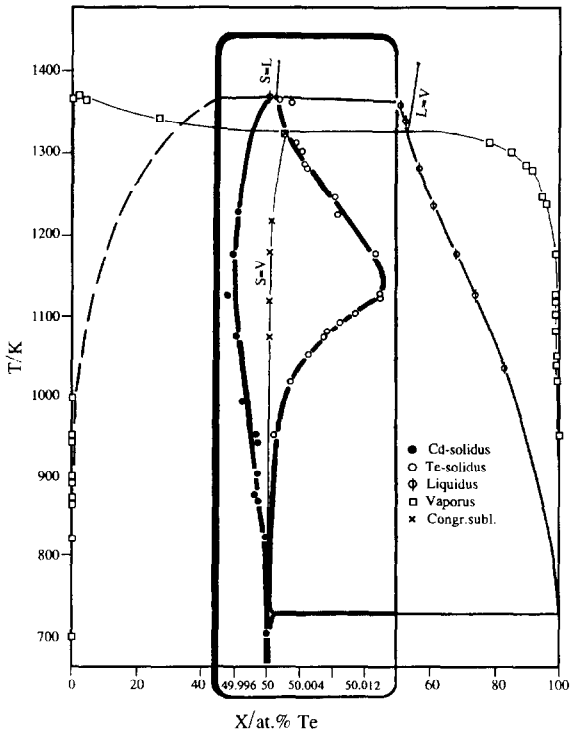

Fig. 3. T–X projection of the CdTe diagram [12]. Near-solidus region is given on an enlarged scale.

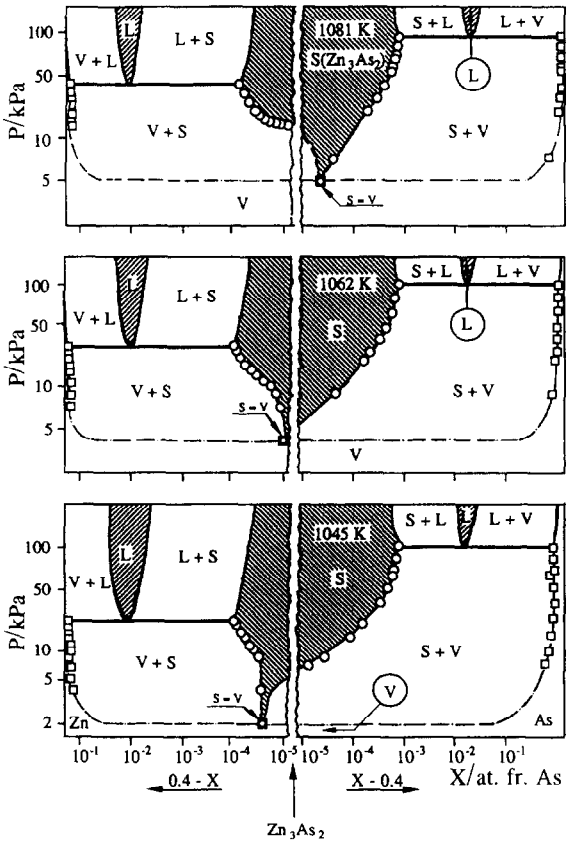

Fig. 4. Isothermal cross sections of the β-Zn_3As_2 solidus [15]: S – β-Zn_3As_2; L – liquid; and V – vapor. Dash-dot line is for vaporus.

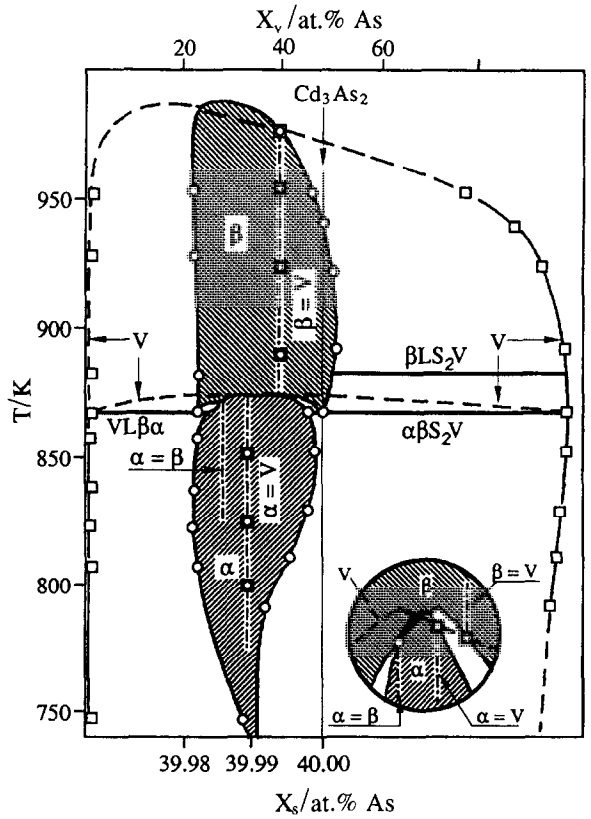

Fig. 5. *T–X* projection of the single phase α-and β-Cd_3As_2 [16]. The inset is a close-up of the α–β phase transition: S_2 – $CdAs_2$; L – liquid; and V — vapor. The order of phases in four phase equilibria βLS_2V, $\alpha\beta S_2V$ and $VL\beta\alpha$ follows the increase in As content in phases.

proved to be independent of temperature (within the possibilities of the experiment), although not exactly stoichiometric: 39.989 at.% As for α-Cd_3As_2 and 39.991 at.% As for β-Cd_3As_2.

3. Conclusion

Principles of a direct method of high precision determination of the equilibrium composition of crystalline solids have been discussed. Vapor-pressure scanning was used to study non-stoichiometry of solids with diverse chemical and phase behaviour: with single-component (YBCO) and multispecies two-component (CdTe) vapors; with different types of sublimation pattern (congruent and incongruent sublimation); with the congruent sublimation composition independent of temperature (Cd_3As_2) and temperature dependent (CdTe and Zn_3As_2); with the stoichiometric plane inside (CdTe) and outside the single-phase solidus volume (α-Cd_3As_2). An extensive vapor-pressure study of the oxygen non-stoichiometry in $YBa_2Cu_3O_y$ as a function of temperature and oxygen pressure is presented, so also the range of non-stoichiometry and some peculiarities of the solidus in II–V and II–VI semiconductors. The reported data constitute a thermodynamic basis for creating certain crystal growth strategies for non-stoichiometric materials and assessing the results. With the *P–T–X* data taken as a standard, vapor-pressure scanning can be used as a powerful analytical tool for precise determination of non-stoichiometry of inorganic materials.

Acknowledgements

This work was done in collaboration with Dr. V.N. Guskov, Dr. I.V. Tarasov, Dr. G.D. Nipan and Professor V.B. Lazarev of the Kurnakov Institute of General and Inorganic Chemistry, Russian Academy of Sciences, Moscow, Russia. The author is grateful to professor L. Ben-Dor of The Hebrew University of Jerusalem for cooperation and support.

References

[1] J.H. Greenberg and V.B. Lazarev, in: E. Kaldis (Ed.), Current Topics in Materials Science, Vol. 12, North-Holland, Amsterdam, 1985, p.119.
[2] V.N. Guskov, J.H. Greenberg and V.B. Lazarev, Proc. Rus. Ac. Sci., 292 (1987) 651.
[3] V.N. Guskov, I.V. Tarasov, V.B. Lazarev and J.H. Greenberg, J. Solid State Chem., 119 (1995) 62.
[4] I.V. Tarasov, V.N. Guskov, V.B. Lazarev, O.V. Shebershneva and M.L. Kovba, Vapor Pressure of $YBa_2Cu_3O_y$, Experimental Data, VINITI Publ., Moscow, 1993.
[5] T.B. Lindemer, J.F. Hunley, J.E. Gates, A.L. Sutton, J. Brynestad, C.R. Hubbard and P.K. Gallagher, J. Amer. Ceram. Soc., 72 (1989) 1775.
[6] K. Kishio, K. Suzuki, T. Hasegawa, T. Yamamoto and K. Kitazawa, J. Sol. State Chem., 82 (1989) 192.
[7] S. Yamaguchi, K. Terabe, A. Saito, S. Yahagi and Y. Iguchi, Jpn. J. Appl. Phys., 27 (1988) L179.
[8] P. Strobel, J.J. Capponi and M. Marezio, Solid State Commun., 64 (1987) 513.

[9] E.D. Specht, C.J. Sparks, A.G. Dhere, J. Brynestad, O.B. Cavin, D.M. Kroeger and M.A. Oye, Phys. Rev. B: Cond. Matter, 37 (1988) 7426.
[10] V.B. Lazarev, K.S. Gavrichev, V.E. Gorbunov and J.H. Greenberg, Thermochim. Acta, 174 (1991) 27.
[11] J.H. Greenberg, V.N. Guskov and V.B. Lazarev, Mat. Res. Bull., 27 (1992) 997.
[12] J.H. Greenberg, J. Crystal Growth, 161 (1996) 1.
[13] J.H. Greenberg, V.N. Guskov, V.B. Lazarev and O.V. Shebershneva, J. Solid State Chem., 102 (1993) 382.
[14] P. Goldfinger and M. Jeunehomme, Trans. Faraday Soc., 59 (1963) 2851.
[15] V.N. Guskov, J.H. Greenberg, V.B. Lazarev and A.A. Kotlyar, Rus. J. Inorgan. Mat., 23 (1987) 1418.
[16] G.D. Nipan, J.H. Greenberg, V.B. Lazarev and M.Y. Zelvenski, Rus. J. Inorgan. Mat., 25 (1985) 1947.